J. Biochem. 123, 790-797 (1998)

Interaction and Orientation of an α-Aminoisobutyric Acid- and Tryptophan-Containing Short Helical Peptide Pore-Former in Phospholipid Vesicles, as Revealed by Fluorescence Spectroscopy[1]

Masood Jelokhani-Niaraki,[2] Kenichi Nakashima, Hiroaki Kodama, and Michio Kondo[3]

Department of Chemistry, Faculty of Science and Engineering, Saga University, Saga 840-8502

Received for publication, September 16, 1997

The interaction and orientation of a membrane protein ion channel model, an α-aminoisobutyric acid analogue of gramicidin B (GBA), in egg yolk phosphatidylcholine vesicles was studied by means of fluorescence spectroscopic techniques. GBA helices form stable ion-conducting pores in membranes [Jelokhani-Niaraki *et al.* (1995) *J. Chem. Soc. Perkin Trans.* 2, 801-808]. In an α-helical model for the peptide, all Trp residues (intrinsic fluorophores) are distributed near the C-terminus. Fluorescence quenching experiments revealed the exposure of the helical peptides' C-termini to aqueous environments. Dansyl-labeled vesicles were used to investigate the GBA dynamism of the interaction with membranes. It was shown that considerable amounts of peptide reside on and in the vicinity of the outer surface of lipid bilayers. The transmembrane transfer to the inner layer is slow due to the high affinity of Trp residues for bilayer interfaces which anchor the peptide to the outer surface. A structural-functional interpretation of the GBA interaction with membranes is presented.

Key words: fluorescence quenching, gramicidin B Aib analogue (GBA), helical peptide pore-former, peptide-lipid interaction, vesicle surface adsorption.

Protein ion channels and pores, normally large macromolecules, authentically interact with biological lipid bilayers, and form gateways for ions and molecules of different sizes to pass through the cell membrane. The intermembrane sections of protein channel and pore structures normally adopt the common secondary structures, *i.e.* α-helices and β-sheets, the former being much more widespread (*1-3*).

One way to model the helical transmembrane segments of protein pore-formers and to investigate their functional properties is to use simple natural and synthetic helical peptides (*4*). Gramicidin and alamethicin, and various natural and synthetic analogues of them, as well as synthetic amphiphilic helical peptides have been used for this purpose in the last two decades (*5-7*). Peptaibols, such as alamethicin, are natural α-aminoisobutyric acid (Aib)-containing peptides that form stable helical secondary structures in a variety of environments. These peptides are considered to be candidates for modeling of the barrel-stave pore structures in lipid bilayers (*8*). The helical stability of peptaibols is basically due to the presence of Aib, an unusual amino acid that induces 3_{10}- and α-helical structures in peptides (*9, 10*).

Tryptophan (Trp), with its amphiphilic character and affinity for lipid bilayer surfaces through both nonpolar and polar interactions, may act as a transmembrane super-secondary structure stabilizer (*11, 12*). Trp residues are located in a variety of membrane proteins near the bilayer surfaces (*13-15*). It has been suggested that the Trp microdipole (~2 Debye), as well as its hydrophobic part, can stabilize the overall transmembrane structures of certain protein pore formers, such as gramicidin and porins, through interactions with lipid bilayer surfaces (*14, 15*).

We have used Trp and/or Aib to design stable functional helical pore-forming synthetic peptides to model membrane protein ion conducting segments (*16, 17*). Aib induces stable helical local structures in the peptide backbone; whereas Trp, when situated near the helical peptide termini, may promote the stability of transmembrane tertiary structures through interhelical packing effects and peptide-lipid interactions. The interaction of an Aib- and Trp-containing peptide pore-former, a gramicidin B Aib analogue (GBA), in lipid bilayers is examined in this study. GBA preserves the basic primary structure of a gramicidin B molecule in which all D-amino acids are replaced by Aib (Fig. 1). The gramicidin analogue takes on rigid helical structures in lipid vesicles, and organic and aqueous solvents (*16*). Moreover, GBA forms stable tight pores in lipid bilayers despite its short length (2.4 nm for a 16 residue α-helix) to span the membrane (average, 3-4 nm) (*16*).

[1] Part of this work was presented in the 24th European Peptide Symposium, Edinburgh (September 1996).

[2] Present address: Protein Engineering Network of Centres of Excellence (PENCE), 713 Heritage Medical Research Centre, University of Alberta, Edmonton, Alberta, Canada T6G 2S2.

[3] To whom correspondence should be addressed. Tel: +81-952-28-8550, Fax: +81-952-28-8458, E-mail: michio@cc.saga-u.ac.jp.

Abbreviations: Aib, α-aminoisobutyric acid; CD, circular dichroism; dansyl-DHPE, *N*-(5-dimethylaminonaphthalene-1-sulfonyl)-1,2 dihexadecanoyl-*sn*-glycero-3-phosphoethanolamine, triethylammonium salt; EYPC, egg yolk phosphatidylcholine; GA, gramicidin A; GBA, gramicidin B Aib analogue; LUV, large unilamellar vesicles; SUV, small unilamellar vesicles; Tris, tris(hydroxymethyl)aminomethane; THF, tetrahydrofuran.

Gramicidin B: Formyl-L-Val-Gly-L-Ala-D-Leu-L-Ala[5]-D-Val-L-Val-D-Val-L-Trp-D-Leu[10]-L-Phe-D-Leu-L-Trp-D-Leu-L-Trp[15]-Glyol

Gramicidin B Aib Analogue: Formyl-L-Val-Gly-L-Ala-Aib-L-Ala[5]-Aib-L-Val-Aib-L-Trp-Aib[10]-L-Phe-Aib-L-Trp-Aib-L-Trp[15]-Glyol

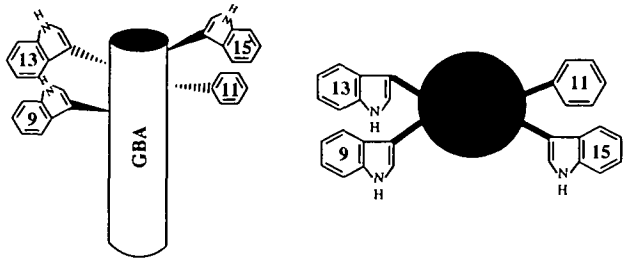

Fig. 1. **Primary structures of the peptides, and a schematic representation of the relative locations of aromatic side chains in the GBA α-helix, shown as a cylinder (lower left) and as a cross-section seen from the N-terminus (lower right) (numbers on aromatic side-chains indicate the residue numbers in the primary structure of the peptides).**

The α-helical model for GBA assumes that the aromatic residues (three Trps and a Phe), located near the C-terminus, are distributed in a pseudo-symmetric manner with Trp 9 and Trp 13 on one side, and Phe 11 and Trp 15 on the other, as shown in Fig. 1.

The bilayer surface oriented helical Aib-containing peptides with Trp residues located in the vicinity of their termini can act as potential protein pore-forming unit mimics with moderate conductance comparable to that of elaborate membrane proteins. In the present study, we employ fluorescence spectroscopic methods to investigate the structure and orientation of GBA molecules in phosphatidylcholine vesicles, using Trp residues at the C-terminus end of the peptide as intrinsic fluorophores. Fluorescence quenching strategies are effectively used for investigating the relative orientation and the degree of exposure of GBA in membranes. Moreover, energy transfer from Trp residues to dansyl-labeled lipids is employed to study the dynamic aspects of GBA-lipid bilayer interactions. A further interpretation of the structure-function relation of GBA in lipid membranes, in addition to what has been discussed previously (*16*), is presented on the basis of the results of fluorescence studies.

MATERIALS AND METHODS

Reagents—GBA was synthesized and purified in a previous study (*18*). Gramicidin A (GA) was from Fluka (>90% GA). Egg yolk phosphatidylcholine (EYPC) (100 mg/liter chloroform solution) was from Sigma. *N*-(5-Dimethylaminonaphthalene-1-sulfonyl)-1,2 dihexadecanoyl-*sn*-glycero-3-phosphoethanolamine, triethylammonium salt (dansyl-DHPE), was from Molecular Probes. All other reagents were of reagent grade and used without further purification. The ethanol used in the fluorescence measurements was of spectroscopic grade. Water was deionized.

Vesicle Preparation—Large unilamellar vesicles (LUV) were prepared with a small-volume extrusion LiposoFast apparatus (Avestin, Canada) using 100 nm pore filters (average diameter of liposomes, 70-80 nm), as described previously (*19*). The initial concentration of EYPC lipids was 3.5 mM (average mol. wt., 750) in Tris-HCl buffer (10 mM, pH 7.4) throughout the experiments. Liposomes were stable for at least a week when stored at 4°C.

Symmetrically labeled EYPC vesicles were prepared by initial mixing of dansyl-DHPE and EYPC chloroform solutions in a 1:10 molar ratio. LUV were then prepared through the hydration of dried lipid films in buffer as described above.

Asymmetrically labeled EYPC vesicles were prepared by the addition of a dansyl-DHPE lipid solution in tetrahydrofuran (THF) (5 mM) to a suspension of EYPC vesicles (3.5 mM) in a 1:20 molar ratio. Due to the slow lipid flip-flop rate during the course of experiments (within 30 min to 1 h after preparation of the labeled vesicles) the majority (80%) of the labeled lipids reside on the outer layer of the vesicles, thus producing an asymmetrical distribution of the chromophore in the inner and outer vesicle monolayers (*20*).

Small unilamellar vesicles (SUV) were prepared by sonication with a probe sonicator, as described previously (*16*).

Sample Preparation—GBA was used as an ethanolic stock solution (0.7 mM), and diluted accordingly in aqueous solvents. The alcohol/water (or aqueous buffer) ratio was 1:200 (v/v) in all experiments. Samples for fluorescence quenching measurements were routinely prepared by adding the desired amount of a quencher to a solution containing constant amounts of the peptide and vesicles. For fluorescence energy transfer measurements, appropriate amounts of dansyl-labeled or dansyl-free vesicles were added to solutions containing a fixed amount of the peptide. The GBA/lipid molar ratio was 1:100 throughout the experiments. Due to their hydrophobicity and the fluorescence intensities at different peptide to lipid ratios, and in accordance with concentration-dependent CD measurements (data not shown), GBA molecules are totally combined with liposomes in a 1:100 molar ratio.

Instrumentation—Fluorescence spectra were measured with a Hitachi F-4000 spectrofluorimeter in cuvettes of 1 cm pathlength, as described previously (*21-23*). The excitation and emission bandpasses were both 5 nm. The fluorescence lifetimes were recorded, using a time-correlated single photon counting method, on a Horiba NAES 1100 nanosecond time-resolved spectrofluorimeter. Emission in lifetime measurements was monitored through a Toshiba UV-34 cut-off filter. Excitation for both steady-state and time-resolved measurements was at 280 nm. As both acrylamide and iodate ion quenchers absorb at this excitation wavelength, the data are corrected for the inner filter effect (*24*).

Fluorescence Quenching Analysis—In general terms, quenching mechanisms can be interpreted as either static or dynamic, and sometimes a combination of both (*24-26*). These mechanisms are formalized in the following equations:

$$\text{Static quenching} \quad F_0/F = 1 + K_s[Q];\ \tau_0/\tau = 1 \quad (1)$$

$$\text{Dynamic quenching} \quad F_0/F = 1 + K_{sv}[Q] = \tau_0/\tau \quad (2)$$

where F_0, F, τ_0, and τ are the fluorescence intensities and lifetimes in the absence and presence of a quencher, respectively. Q represents the quencher. K_s is the static quenching constant, which can be interpreted as the equi-

librium constant of the complex between the quencher and the probe prior to excitation. K_{sv} is the dynamic quenching constant, often termed the Stern-Volmer constant.

A linear curve in the plot of F_0/F *vs.* [Q] (Stern-Volmer plot), fulfilling the conditions in Eq. 2, indicates a dynamic quenching mechanism. However, in many cases the curve in a Stern-Volmer plot shows some deviation, which makes the interpretation less straightforward. Upward positive deviation of the curve was observed in all of the experiments in this study. If the $\tau_0/\tau = 1$ condition in Eq. 1 is held, the quenching is basically static and the equilibrium constant can be calculated from the F *vs.* [Q] curve at 50% quenching: $K_s = 1/[Q]_{50}$. However, a concentration-dependent lifetime ratio implies a combined static-dynamic mechanism for the quenching. Modified Stern-Volmer plots can account for the latter combined mechanism:

Modified Stern-Volmer Equation

$$F_0/Fe^{V[Q]} = 1 + K_{sv}[Q] = \tau_0/\tau \quad (3)$$

where V is the static constant. V is different from K_s in that it can account for weak associations between the fluorophore and the quencher. V represents the active volume around the excited fluorophore, in which the presence of a quencher may cause instantaneous quenching at the time of excitation. Non-exponential rapid decay can also occur in this sphere of action due to time-dependent diffusion processes. This transient effect is mostly observable in viscous environments and is normally not included in the modified Stern-Volmer equation (*26*).

RESULTS

The fluorescence spectra of GBA in three environments are shown in Fig. 2. The emission with the highest intensity was seen in ethanol despite that the absorbance of GBA at 290 nm (for excitation of the ethanolic solution) is lower than that at 280 nm (for excitation of the others). The GBA spectrum in EYPC liposomes was considerably more intense than that in buffer. In spite of their negligible relative shifts (all maxima around 340–342 nm), the maximum emission values showed a considerable blue shift when compared to Trp in aqueous environments (around 350 nm).

Table I shows the fluorescence lifetimes of GBA in various environments compared to those of Trp and GA. Since the fluorescence of these compounds shows a double exponential decay profile in all the solvents employed (each component is not shown), we have introduced an averaged lifetime, $\langle\tau\rangle$:

$$\langle\tau\rangle = \Sigma\alpha_i\tau_i^2/\Sigma\alpha_i\tau_i. \quad (4)$$

As it was not a purpose of the present study to elucidate the nature of decay curves, we will not be concerned with the details of each decay component. We use the averaged

TABLE I. **Fluorescence lifetimes of Trp, GA, and GBA in different environments at 25°C.**

Solvent	Compound	$\langle\tau\rangle$/ns[a]	χ^{2}[b]
Ethanol	Trp	3.22	0.94
	GA	3.74	1.06
	GBA	4.08	1.27
Ethanol/water	Trp	2.60	1.01
(1/1: v/v)	GA	4.35	1.17
	GBA	5.32	1.31
Tris-HCl buffer	Trp	2.73	1.00
(10 mM, pH 7.4)	GA	3.74	1.42
	GBA	3.39	1.30
EYPC in Tris-HCl buffer[c]	Trp	2.86	0.95
	GBA	5.55	1.06

[a]Average lifetime calculated in accordance with: $\langle\tau\rangle = \Sigma\alpha_i\tau_i^2/\Sigma\alpha_i\tau_i$, where α_i and τ_i represent the pre-exponential factor and lifetime of the ith component, respectively; [b]Least-square curve fitting value as a criterion for goodness of fit; [c]the molar ratios of Trp/lipid and GBA/lipid were 1:35 and 1:100, respectively.

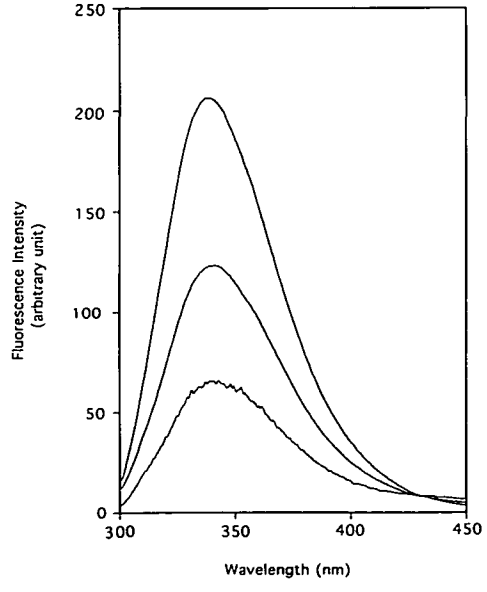

Fig. 2. **Fluorescence emission spectra of GBA (3.5 μM) in ethanol (upper trace), large unilamellar EYPC vesicles (350 μM) in Tris-HCl buffer (middle trace), and Tris-HCl buffer (lower trace) at 25°C; excitation was at 290 nm for ethanol, and 280 nm for vesicles and buffer.**

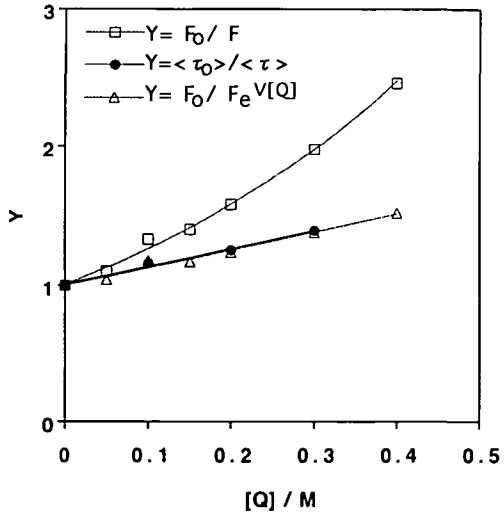

Fig. 3. **Stern-Volmer and modified Stern-Volmer plots for the quenching of GBA (3.5 μM) fluorescence by acrylamide in large unilamellar EYPC vesicles (350 μM) in Tris-HCl buffer at 25°C.** Excitation was at 280 nm, and emission was monitored at 342 nm. The samples were stored in the dark for 30 min prior to the fluorescence measurements.

lifetime, $\langle\tau\rangle$, in the later discussion of the results of lifetime measurements. In general, GBA has longer or comparable (in one case) average lifetimes in aqueous and nonaqueous milieus.

In order to assess the interaction and orientation of GBA molecules in lipid environments, two series of experiments were performed. In the first series, three aqueous quenchers of Trp (neutral, negatively charged, and positively charged) were used to study the relative orientation and location of GBA in neutral EYPC vesicles. In the second series, symmetrically and asymmetrically dansyl-labeled EYPC vesicles were employed to investigate some dynamic aspects of the interaction of GBA with and within lipid bilayers. The results are used for interpretation of the GBA structure and function in membranes.

Figure 3 shows a Stern-Volmer plot and its modified form for fluorescence quenching of GBA in liposomes by acrylamide. Acrylamide is an efficient quencher of indole and Trp (*25*). The main plot has an upward bend, reflecting the involvement of both static and dynamic mechanisms. The Trp and protein fluorescence quenching by acrylamide, and the mechanisms involved have already been studied in detail (*25, 26*). A modified Stern-Volmer plot (Eq. 3) was used to separate the static and dynamic parts of the quenching. The static quenching constant, V, was estimated to be 1.20 M^{-1} (radius of active volume, ~0.78 nm). The modified and $\langle\tau_0\rangle/\langle\tau\rangle$ plots were superimposed to yield a dynamic constant, K_{sv}, of 1.28 M^{-1}. The bimolecular quenching constant, K_q, was calculated to be 2.53×10^8 $M^{-1}\cdot s^{-1}$ ($K_q = K_{sv}/\langle\tau_0\rangle$).

Figure 4 shows the quenching of GBA in liposomes by IO_3^- ions (KIO_3). The modified Stern-Volmer plot became linear, and was superimposed on the $\langle\tau_0\rangle/\langle\tau\rangle$ plot. The value calculated for V was 1.25 M^{-1} (radius of active volume, ~0.79 nm). The K_{sv} constant calculated from the $\langle\tau_0\rangle/\langle\tau\rangle$ plot was 0.57 M^{-1} ($K_q = 1.12\times10^8$ $M^{-1}\cdot s^{-1}$).

Interestingly, a different quenching mechanism can be attributed to the interaction between Cu^{2+} ions ($CuSO_4$) and GBA in lecithin liposomes. This is shown in Fig. 5. The $\langle\tau_0\rangle/\langle\tau\rangle$ plot showed a constant value for the lifetime of GBA fluorescence (inset) in the whole quencher concentration range, implying a static mechanism of the complex formation (Eq. 1) (*24*). The K_s for this plot was 3,616 M^{-1}, which gives an apparent $K_q = 7.12\times10^{11}$ $M^{-1}\cdot s^{-1}$.

The second series of experiments involved time-dependent fluorescence methodology. Figure 6 shows a two-phase process for the interaction of GBA with symmetrically dansyl-DHPE labeled liposomes. The dansyl fluorophore was located at water-vesicle interfaces. In the first 10 min the time-dependent course of the interaction showed a

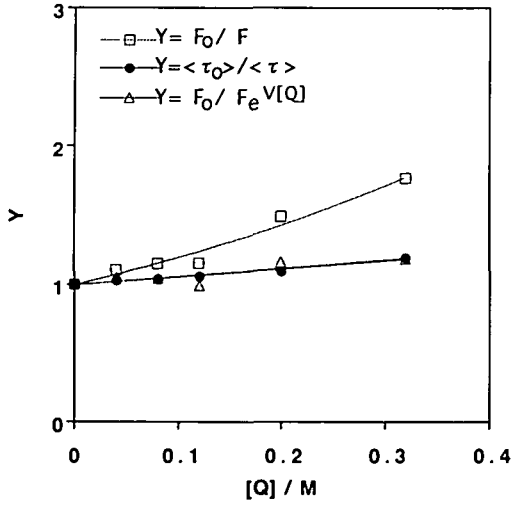

Fig. 4. **Stern-Volmer and modified Stern-Volmer plots for the quenching of GBA (3.5 μM) fluorescence by IO_3^- ions in large unilamellar EYPC vesicles (350 μM) in Tris-HCl buffer at 25°C.** The experimental conditions were as in Fig. 3.

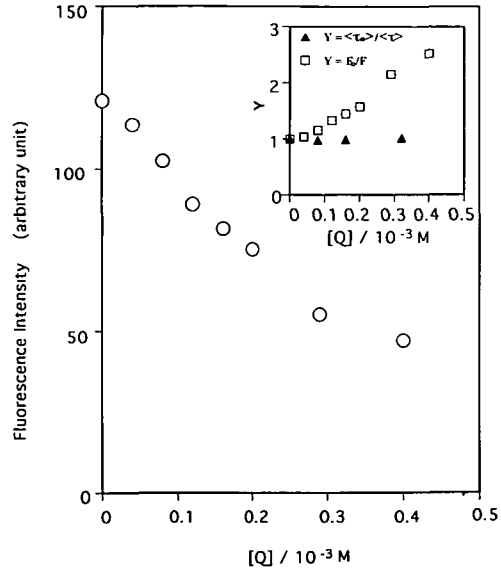

Fig. 5. **A plot of GBA (3.5 μM) fluorescence intensity *vs.* Cu^{2+} concentration in large unilamellar EYPC vesicles (350 μM) in Tris-HCl buffer at 25°C.** The inset shows the Stern-Volmer plots; the experimental conditions were as in Fig. 3.

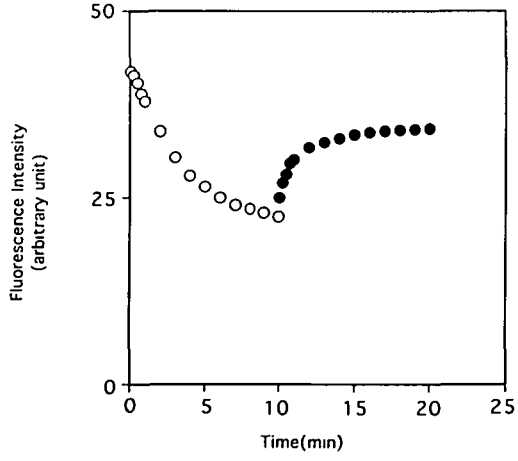

Fig. 6. **Time-dependent interaction of GBA (3.5 μM) with symmetrically dansyl-labeled large unilamellar EYPC vesicles (350 μM) in Tris-HCl buffer at 25°C.** Open circles represent the decrease in GBA fluorescence emission (monitored at 340 nm) upon interaction with dansyl-labeled liposomes; closed circles represent the gradual increase in GBA emission intensity upon interaction of the peptide with a new population of dansyl-free liposomes (5 times in excess), added 10 min after the initial mixing of GBA with dansyl-labeled liposomes; excitation was at 280 nm.

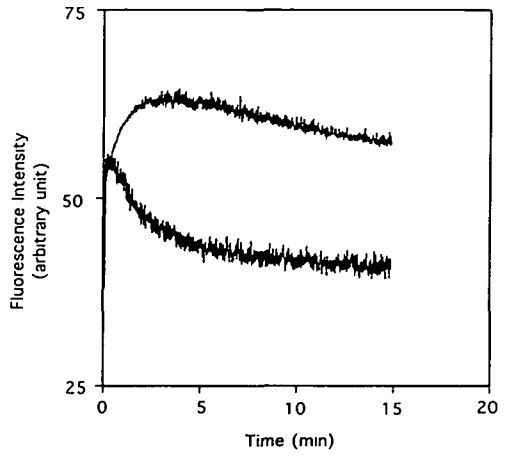

Fig. 7. **Time-dependent interaction of GBA (3.5 μM) with asymmetrically dansyl-labeled large unilamellar EYPC vesicles (350 μM) in Tris-HCl buffer at 25°C.** The upper and lower traces represent the fluorescence emission of dansyl (monitored at 520 nm) and Trp residues in GBA (monitored at 340 nm), respectively; the experimental conditions were as in Fig. 6.

constant decrease in fluorescence due to nonradiative energy transfer from GBA Trp residues to dansyl-labeled lipids. As the adsorption of peptides onto liposomes usually takes place very quickly, the gradual decrease (~10 min) in GBA fluorescence might reflect an orientational change of GBA (and/or a peptide-peptide interaction) on the lipid surface. After 10 min, a new population of dansyl-free EYPC liposomes was added in a considerable excess (5 times molar ratio). The fluorescence intensity showed a notable, but gradual, increase after another 10 min, but did not return to the level at the beginning of the experiment. The interaction of Trp and dansyl moieties was clearly weakened by the addition of dansyl-free vesicles through the redistribution of GBA among liposomes.

Figure 7 shows the interaction of GBA with asymmetrically dansyl-DHPE labeled vesicles. In these vesicles the majority of dansyl-labeled lipids were distributed on the outer surface of the liposomes. In one experiment, the decay of GBA fluorescence due to energy transfer to dansyl was monitored for 15 min. In another experiment, the increase in dansyl fluorescence due to the acceptance of energy from GBA was monitored for 15 min. The presentation of these traces as one plot can illustrate part of the molecular phenomenon occurring on the outer surface of or within the lipid bilayer. As the critical energy transfer distance between Trp and dansyl was estimated to be about 2 nm, in accordance with Förster theory (*20*), any considerable dynamic change in the distance between the energy donor-acceptor pair might be reflected in both the Trp and dansyl time-dependent emission patterns. This assumption will be used to reach to some qualitative conclusions related to the behavior of GBA in membranes.

DISCUSSION

In accordance with one of the hydrophobicity scales (*27*), GBA is a hydrophobic peptide with an average hydrophobicity of 0.75 and a hydrophobic moment of 0.076 (the hydrophobicity value for Aib was assumed to be an average of the Ala and Val hydrophobicities) (*4*). Due to its hydrophobicity and the presence of Trp residues the peptide exhibits a high affinity for membrane surfaces (*11, 12*). The intermolecular reaction of GBA molecules within lipid bilayers has already been investigated by means of CD measurements (*16*). It is assumed that GBA forms tight barrel-stave shaped pores in membranes upon the appliance of transmembrane potential, and that ions pass through these pores. The moderate conductance of GBA pores is mostly in the range of protein ion channels (*16*).

A two-stage model accounts for the stability and assembly of integral protein α-helices in membranes (*28*). In the first stage, hydrophobic helices interact with membranes through a hydrophobic effect and then become thermodynamically stabilized through strengthening of their intramolecular hydrogen bonds. In the second stage, after reaching equilibrium in lipid environment, the helical peptides further interact through non-hydrophobic forces to form peptide assemblies which can have functional roles, and may dictate the rest of the folding process of membrane proteins (*28*). In addition, discrete hydrophobic and amphipathic α-helices may be autonomously assembled on lipid membrane surfaces or in their hydrophobic interior (*28, 29*). The assembly of helical peptides on the surface of some lipid bilayers may have an overall stabilizing effect by reducing the negative monolayer curvature strain (*30*). On the other hand, transmembrane barrel-stave shaped self-association of helical peptides can promote the lysis of cells or vesicles directly, by forming pores with large diameters (*e.g. 31, 32*), or indirectly, by forming small ion channels for the ions to leak through, leading to osmotic lysis (*30*).

As can be observed in Fig. 2, GBA fluorescence in the buffer was much weaker than that in vesicles and alcohol. In comparison with the maximum emission of Trp in aqueous solutions, the blue-shifted maximum emission of GBA in three different solvent systems implies more hydrophobic environments around Trp residues in all three milieus. Interestingly, GBA adopts three different structures in these solvents, as revealed by CD spectra (*16*). The structural change can be also detected by monitoring the fluorescence lifetimes in these environments (*vide supra*, Table I). The shortest average lifetime for GBA was observed in buffer. Despite the difference in structure (*16*), the GBA fluorescence lifetimes in vesicles and 50% ethanol were comparable, and longer than that in pure ethanol. The blue-shift of the spectra of GBA implies a hydrophobic microenvironment for Trps in aqueous solutions, which could be a result of partial aggregation of the GBA molecules. However, in liposomes the blue-shift could mean an overall structural change [also observable in CD spectra (*16*)] due to adsorption and partial incorporation of the fluorophores on and into the lipid surface and interior.

Figures 3-5 show that the GBA fluorescence in liposomes was quenched through different mechanisms, depending on the nature of the quencher (*i.e.* neutral, negatively, or positively charged). This is in contrast to the cases of lipid-free solutions, in which quenching of the GBA fluorescence is due to a dynamic process for any of the three quenchers. Despite the different mechanisms, however, the fluorescence quenching results for all three types of quenchers in the vesicles imply that a considerable amount of Trp residues at the C-terminus of GBA are exposed to aqueous environments. In the case of acrylamide (Fig. 3),

the contributions of the static and dynamic parts of the quenching mechanism are almost the same ($1.20\ M^{-1}$ *vs.* $1.28\ M^{-1}$, respectively). However, it should be noted that we are dealing with a group of three Trps (Phe is excluded as it is not influential in emission, but it possibly interacts with its Trp neighbors), which makes the system more complex. The reported values of V for indole derivatives and Trp- containing peptides' fluorescence quenching by acrylamide are mostly in the range of $1\text{-}3\ M^{-1}$ (*25, 33*). The value of K_q in this fluorescence quenching system is 2 orders of mag- nitude less than the values suitable for a dominantly diffusion-controlled collision. This can be partly accounted for by the slow diffusion rate of vesicles ($6.10\times10^{-8}\ cm^2\cdot s^{-1}$ for a sphere of 80 nm diameter) with peptides adsorbed on their exterior surfaces. During quenching, acrylamide collides with these giant liposomes, but is unlikely to enter their hydrophobic interior (*25*).

In comparison with acrylamide, the IO_3^- quenching of GBA (Fig. 4) shows a similar value for the static quenching, but less than half the value for the dynamic quenching. Here, the smaller slope of the lifetime ratio plot implies less contribution by the collisional quenching and more contribution by the static quenching. This difference in the collisional quenching values of the quenchers might be due to partial electrostatic interaction of IO_3^- ions with the lipid bilayer surface, as is the case with other charged ions (*25, 26*). Another cause for this disagreement could be that the transient part of the diffusion process is often neglected in the modified Stern-Volmer equation (*26*). This transient part becomes especially important in viscous environments, in this case lipid bilayer interfaces and hydrophobic parts.

The quenching of GBA fluorescence by Cu^{2+} ions (Fig. 5) is more straightforward and is best resolved by considering a complex-forming static mechanism, as the fluorescence lifetime remains constant. The apparent K_q for this quenching system is an order of magnitude greater than the common values for diffusion-controlled reactions. Cu^{2+} ions possibly quench peptide Trps located on the surface of vesicles by forming non-fluorescent complexes.

An interpretation of the data shown in Fig. 6 is that a considerable amount, but not all, of the GBA molecules is transferred to added dansyl-free vesicles. On the transfer of peptides to the newly added large excess of unlabeled vesicles, the distance between Trp and dansyl increases, and the energy transfer becomes less effective and fades away (hence, increase in the fluorescence intensity). This phenomenon occurs in the same manner, but faster, when dansyl-free vesicles are added at shorter time intervals (data not shown). The ease of peptide transfer among vesicles, even 10 min after the initial mixing of the peptide and liposomes, indicates that a considerable amount of the peptide molecules resides loosely on the outer surface of vesicles at this time, and thus not many are incorporated deeper or transferred to the inner membrane layer.

As shown in Fig. 7, GBA interacts with outer-layer labeled EYPC molecules in a dynamic manner. An initial sharp decrease and increase in the Trp and dansyl emissions, respectively, are expected. Peptides approach the bilayer surfaces and interact with dansyl-labeled lipids, and then energy transfer occurs. Following the traces after this initial phase (continuing for ~2 min after the initial mixing of the peptide and liposomes) can reveal further peptide-lipid interactions. The Trp emission decline continues and becomes reasonably constant after 15 min. If a considerable amount of the peptides was transferred to the inner layer, we would have expected an increase in the Trp emission decay trace. The transmembrane transfer causes an increase in the distance between the Trp and dansyl (mostly distributed on the outer layer) moieties, and if this separation increases to more than the critical energy transfer distance (2 nm, almost the length of a lipid monolayer) the energy transfer decreases considerably. In the latter case, the fluorescence of Trp should be somehow revived as it can not effectively transfer energy to the dansyl moiety. Such an increase, or a change in the emission decay pattern is not observed. In contrast, the data show a constant decrease in the Trp fluorescence. Moreover, the dansyl emission trace shows a gradual decrease after the initial phase, it becoming relatively constant after 15 min. The reason for this latter decrease is presently unclear. One possible explanation is that a peptide-peptide interaction takes place on the surface of membranes, which not only makes Trp residues less accessible for interaction with dansyl-labeled lipids distributed on the water-vesicle interface, but also causes self-quenching of the Trp fluorescence due to the reduced distance between Trp residues. The helix-helix interaction has already been suggested for GBA in vesicle systems, by CD studies (*16*). This interaction causes red-shifts and changes in the intensities of the minima (at around 208 and 222 nm) and the maximum (at around 192 nm) of the CD spectra of typical monomeric α-helical motifs. Corresponding changes were observable in the CD spectra of GBA transferred from alcoholic solvents (monomeric GBA) to phospholipid vesicles (*16*). The intermolecular interaction between peptide molecules may result in partial shielding of Trp residues from the energy transfer. The time-dependent progress of this shielding can cause a constant and gradual decrease in the dansyl emission without causing an increase in the Trp emission intensity. The rate of decrease diminishes considerably after 15 min, indicating an equilibrium for the vesicle surface interactions. It can be assumed that at this point peptide aggregates are formed on or near the interface of the water and liposomes. The most simple aggregates in lipid bilayers are parallel or antiparallel helix dimers (*28*). Lateral packing of monomers through the interlacing effect of Trp residues may yield partially buried or interfacial larger aggregates. These structures can lead to ion conducting pore structures, when a transmembrane potential difference is applied (*16, 34*). The experiments described so far were attempts to further clarify the location and orientation of GBA molecules in lipid bilayers. The results further support our conclusions on the mechanism of pore formation by GBA, described elsewhere (*16, 34*). A general interpretation of the experiments leads to the conclusion that the Trp residues of GBA, located at its C-terminus, are mostly exposed to aqueous environments in EYPC liposomes. As all of these peptides are adsorbed on and incorporated into vesicles, it can be assumed that GBA molecules are located at the water-liposome interface and/or partially incorporated into the lipid bilayer with their C-termini exposed. As a result, GBA is mostly anchored to the outer surface of the bilayer, and thus its transmembrane transfer is likely to be slow. Both fluorescence and previous CD studies (*16*) suggested peptide-peptide inter-

actions, which can cause the formation of interfacial or partly buried peptide aggregates in lipid membranes.

To conclude this report and the previous results of a patch-clamp experiments (*16*), and to get a more detailed picture of ion-conducting behavior of GBA in lipid membranes, a schematic model for the interaction and orientation of GBA in bilayers is presented in Fig. 8. As predicted in the two-stage model (*vide supra*), GBA helices are more stabilized in membranes (see Ref. *16* and Fig. 2 for the fluorescence data), and exhibit signs of aggregation. GBA shows moderate transmembrane dye-leakage in dipalmitoyl phosphatidylcholine vesicles, compared to alamethicin, even at high peptide/lipid molar ratios, suggesting smaller pore sizes or different pore shapes (*35*). GBA aggregation can be interfacial. This means peptides may form antiparallel dimers and aggregates of higher order on the outer surface of vesicles. The major combining force in this case could be interhelical dipole-dipole interactions, as well as hydrophobic effects. GBA aggregation in membranes can also occur in a partially buried form. The helix-helix interaction may occur through the interlacing of aromatic residues located at peptide C-termini. As the C-termini of peptide are oriented towards the membrane interface, the effect of dipole-dipole repulsion of the interacting parallel-oriented helices can be reduced by the dielectric shielding of bulk solvent molecules or lipid polar heads. That is, GBA can form half-buried barrel-stave structures through helix-helix interactions and aromatic side-chain packing effects. The appliance of an electrical potential through membranes can further force these aggregated states to form ion conducting units. Electrophysiological experiments have indicated ion conducting pores mostly composed of 3 or 4 helices (*16*). These results and the ion conducting data further suggested the possibility of the existence of tight, flexible, but stable pores for this relatively short helical peptide.

Finally, the structure and function of the hydrophobic stable helical peptide pore-former, GBA (composed mainly of a special arrangement of Trp and Aib residues), in lipid bilayers will lead to some insight into the modes of interaction of membrane proteins with lipid bilayers, and their physiological functions.

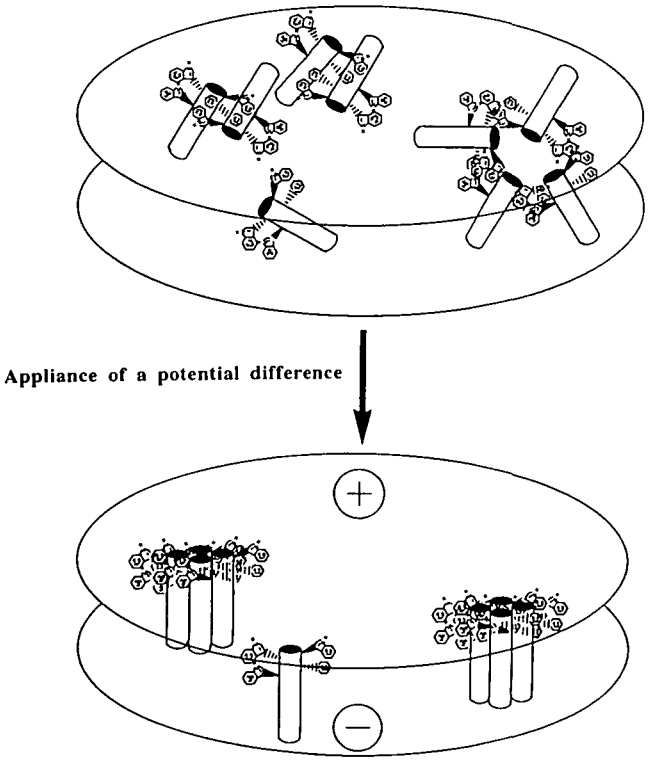

Fig. 8. **Schematic interaction and orientation of GBA molecules in lipid bilayers.** The upper scheme shows some of the possible aggregated states of GBA molecules in the bilayer (Trp residues enhance the peptide adsorption and incorporation processes, and may further stabilize peptide assemblies through interhelical packing effects); the lower scheme shows possible barrel-stave tetrameric pore structures upon the appliance of a potential difference across the bilayer (the electrical field thus applied forces the GBA molecules, shorter than the average bilayer thickness, to form ion-conducting units; this might be accompanied by structural changes in individual helical molecules, shown as longer helices in this case, and/or by changes in the lipid bilayer thickness).

REFERENCES

1. Popot, J.-L. (1993) Integral membrane protein structure: transmembrane α-helices as autonomous folding domains. *Curr. Opinion Struct. Biol.* **3**, 532-540
2. Popot, J.-L., De Vitry, C., and Atteia, A. (1994) Folding and assembly of integral membrane proteins: an introduction in *Membrane Protein Structure: Experimental Approaches* (White, S.H., ed.) pp. 41-96, Oxford University Press, New York
3. Unwin, N. (1989) The structure of ion channels in membranes of excitable membranes. *Neuron* **3**, 665-676
4. Sansom, M.S.P. (1991) The biophysics of peptide models of ion channels. *Prog. Biophys. Mol. Biol.* **55**, 139-235
5. Wallace, B.A. (1990) Gramicidin channels and pores. *Annu. Rev. Biophys. Biophys. Chem.* **19**, 127-157
6. Woolley, G.A. and Wallace, B.A. (1993) Model ion channels: gramicidin and alamethicin. *J. Membr. Biol.* **129**, 109-136
7. Lear, J.D., Wasserman, Z.R., and DeGrado, W.F. (1988) Synthetic amphiphilic peptide models for protein ion channels. *Science* **240**, 1177-1181
8. Boheim, G., Hanke, W., and Jung, G. (1983) Alamethicin pore formation: voltage-dependent flip-flop of α-helix dipoles. *Biophys. Struct. Mech.* **9**, 181-191
9. Burgess, A.W. and Leach, S.J. (1973) An obligatory α-helical amino acid residue. *Biopolymers* **12**, 2599-2605
10. Balaram, P. (1992) Non-standard amino acids in peptide design and protein engineering. *Curr. Opinion Struct. Biol.* **2**, 845-851
11. Jacobs, R.E. and White, S.H. (1989) The nature of the hydrophobic binding of small peptides at the bilayer interface: implications for the insertion of transbilayer helices. *Biochemistry* **28**, 3421-3437
12. Wimley, W.C. and White, S.H. (1993) Membrane partitioning: distinguishing bilayer effects from the hydrophobic effect. *Biochemistry* **32**, 6307-6312
13. Deisenhofer, J. and Michel, H. (1989) The photosynthetic reaction centre from the purple bacterium *Rhodopseudomonas viridis*. *EMBO J.* **8**, 2149-2170
14. Kreusch, A., Neubüser, A., Schiltz, E., Weckesser, J., and Schultz, G.E. (1994) Structure of the membrane channel porin from *Rhodopseudomonas blastica* at 2.0 Å resolution. *Protein Sci.* **3**, 58-63
15. Hu, W., Lee, K.-C., and Cross, T.A. (1993) Tryptophans in membrane proteins: indole ring orientations and functional implications in the gramicidin channel. *Biochemistry* **32**, 7035-7047
16. Jelokhani-Niaraki, M., Kodama, H., Ehara, T., and Kondo, M. (1995) Conformational studies and pore-forming properties of an α-aminoisobutyric acid analogue of gramicidin B. *J. Chem. Soc. Perkin Trans.* **2**, 801-808

17. Kondo, M., Higashimoto, Y., Jelokhani-Niaraki, M., and Kodama, H. (1996) Solid-phase synthesis and conformational analysis of amphiphilic Aib-containing helical peptides in *Proceedings of the 24th European Peptide Symposium 1996 (Edinburgh)*, pp. 545-546
18. Jelokhani-Niaraki, M., Yoshioka, K., Takahashi, H., Kato, F., and Kondo, M. (1992) Changes in conformation and antimicrobial properties caused by replacement of D-amino acids with α-aminoisobutyric acid in the gramicidin backbone: synthesis and circular dichroic studies. *J. Chem. Soc. Perkin Trans.* **2**, 1187-1193
19. MacDonald, R.C., MacDonald, R.I., Menco, B.Ph.M., Takeshita, K., Subbarao, N.K., and Hu, L.-R. (1991) Small-volume extrusion apparatus for preparation of large unilamellar vesicles. *Biochim. Biophys. Acta* **1061**, 297-303
20. Matsuzaki, K., Murase, O., Fujii, N., and Miyajima, K. (1995) Translocation of a channel-forming antimicrobial peptide, Magainin 2, across lipid bilayers by forming a pore. *Biochemistry* **34**, 6521-6526
21. Nakashima, K., Fujimoto, Y., and Anzai, T. (1995) Photoluminescent properties of octadecylrhodamine B in micelles of low-molecular-weight detergents and water-soluble triblock copolymers. *Photochem. Photobiol.* **61**, 592-599
22. Nakashima, K., Fujimoto, Y., and Kido, N. (1995) Fluorescence studies on the adsorption of octadecylrhodamine B onto a latex surface. *Photochem. Photobiol.* **62**, 674-679
23. Nakashima, K. and Kido, N. (1996) Fluorescence quenching of 1-pyrenemethanol by methylviologen in polystyrene latex dispersions. *Photochem. Photobiol.* **64**, 296-302
24. Lakowicz, J.R. (1983) *Principles of Fluorescence Spectroscopy*, Plenum, New York
25. Eftnik, M.R. and Ghiron, C.A. (1976) Fluorescence quenching of indole and model micelle systems. *J. Phys. Chem.* **80**, 486-493
26. Eftnik, M.R. and Ghiron, C.A. (1981) Fluorescence quenching studies with proteins. *Anal. Biochem.* **114**, 199-227
27. Eisenberg, D., Schwarz, E., Komaromy, M., and Wall, R. (1984) Analysis of membrane and surface protein sequences with the hydrophobic moment plot. *J. Mol. Biol.* **179**, 125-142
28. Popot, J.-L. and Engelman, D.M. (1990) Membrane protein folding and oligomerization: the two-stage model. *Biochemistry* **29**, 4031-4037
29. Deber, C.M. and Li, S.-C. (1995) Peptides in membranes: helicity and hydrophobicity. *Biopolymers (Peptide Sci.)* **37**, 295-318
30. Epand, R.M., Shai, Y., Segrest, J.P., and Anantharamaiah, G.M. (1995) Mechanism for the modulation of membrane bilayer properties by amphipathic helical peptides. *Biopolymers (Peptide Sci.)* **37**, 319-338
31. Sansom, M.S.P. (1993) Alamethicin and related peptaibols-model ion channels. *Eur. Biophys. J.* **22**, 105-124
32. Balaram, P., Krishna, K., Sukumar, M., Mellor, I.R., and Sansom, M.S.P. (1992) The properties of ion channels formed by zervamicins. *Eur. Biophys. J.* **21**, 117-128
33. De Kroon, A.I.P.M., Soekarjo, M.W., De Gier, J., and De Kruijff, B. (1990) The role of charge and hydrophobicity in peptide-lipid interaction: a comparative study based on tryptophan fluorescence measurements combined with the use of aqueous and hydrophobic quenchers. *Biochemistry* **29**, 8229-8240
34. Jelokhani-Niaraki, M., Kodama, H., Ehara, T., and Kondo, M. (1995) How a short gramicidin Aib analogue can form pores in phospholipid bilayers in *Peptide Chemistry 1994* (Ohno, M., ed.) pp. 113-116, Protein Research Foundation, Osaka
35. Jelokhani-Niaraki, M. (1995) Studies on structure-function relationship of helical peptide pore-formers in membranes (Ph.D. thesis), Saga University, Saga